AE-398
UDC 539.166.08
539.122.164
539.173.4.162.2

AE-398

Prompt Gamma Radiation from Fragments in the Thermal Fission of ^{235}U

H. Albinsson and L. Lindow

AKTIEBOLAGET ATOMENERGI
STUDSVIK, NYKÖPING. SWEDEN 1970

PROMPT GAMMA RADIATION FROM FRAGMENTS IN THE THERMAL FISSION OF ^{235}U

H Albinsson* and L Lindow

ABSTRACT

Measurements were made on the gamma radiation emitted from fission fragments in slow neutron induced fission of ^{235}U. The fragments were detected with solid state detectors of the surface barrier type and the gamma radiation with a NaI(TI) scintillator. Mass selection was used so that the gamma radiation could be measured as a function of fragment mass. Time discrimination between the fission gammas and the prompt neutrons released in the fission process was employed to reduce the background. The gamma radiation emitted during different time intervals after the fission event was studied with the help of a collimator, the position of which was changed along the path of the fission fragments. In this way a decay curve was obtained from which the life-time of one of the gamma-emitting states could be estimated. The relative yield of the gamma-rays was determined as a function of mass for different gamma-ray energy portions and two specific time intervals after the fission events.

Comparisons were made with data obtained from ^{252}Cf fission. Attention is drawn to some features which seem to be the same in ^{235}U and ^{252}Cf fission.

---

* Chalmers University of Technology, Gothenburg

Printed and distributed in June 1970

LIST OF CONTENTS

1. INTRODUCTION

During recent years much interest has been devoted to the study of the gamma radiation emitted in the de-excitation of fission fragments [1 - 18]. Most of these studies have concerned the K X-ray and conversion electron yields [6 - 9, 12 - 15] in different time intervals within about 100 nanoseconds after the fission event. The main bulk of data have come from experiments with ^{252}Cf spontaneous fission and to a less extent from studies of slow neutron induced fission of ^{235}U [5, 10, 11, 17]. Measurements of the latter fission process are rather difficult to perform because of the severe background always present in reactor experiments. The light mass groups are different in the two fission processes and therefore a close examination of the uranium fission is worthwhile, even if the californium fission may be easier to investigate.

In most fission measurements nowadays mass selection is used and the yields of photons and electrons are studied in coincidence with the fragment masses.

The prompt neutrons which are also released during the fission events cause a background in the gamma detector. In very few cases has the time-of-flight technique been adopted for discrimination between the prompt neutrons and the fission gamma radiation [18 - 22]. At any rate no extensive study with this method has been made so far. To be effective, distances of about 50 cm or more between the fission foil and the gamma detector must be used, giving very small solid angles of the gamma detector and thus also low counting rates.

Of great interest are the life-times of the gamma-emitting states of the fragments. They can be studied by a collimator technique in the following way. The gamma radiation is emitted from fragments

in flight and, by changing the position of a collimator along the path of the moving fragments, one can select different time intervals during which fission gamma radiation is allowed to reach the gamma detector. Such a technique has been used in few experiments up till now: in ^{252}Cf fission [1, 21] and in ^{235}U fission [10, 19]. As the average velocity of a fragment is about 1 cm/ns, a collimator with a slit width of 1 mm will let a fragment be exposed to the gamma detector for a time interval of about 10^{-10} s.

In the present investigation the so-called prompt gamma radiation from fragments in slow-neutron induced fission of ^{235}U was studied. The expression "prompt gamma radiation" used here was coined by Johansson[1]. In his studies of californium fission it was found that the radiation could be divided into two parts: a "prompt" component with a half-life shorter than 10^{-9} s and a "delayed" component. This division is, of course, somewhat arbitrary, but Johansson found a distinct difference in the characteristics of the radiation in the two cases.

2. EXPERIMENTAL PROCEDURE

2.1. Apparatus

The principle of the set-up of this experiment is shown in fig. 1. A neutron beam from the Studsvik R2 reactor was collimated, so that no part of the beam struck more than the target and its mounting frame inside a vacuum chamber. Two solid state detectors of the surface barrier type were placed in parallel and symmetrically around the foil to measure the energies of the fission fragments. The detectors[+] were about 4 cm^2 in area, fabricated from 400 ohmcm n-type silicon and operated at about 70 V bias. The distance between each detector and

[+] Type C7904 Heavy Ion Detectors supplied by ORTEC, Oak Ridge, Tenn., USA

the fissile foil was 2 cm. The gamma detector was a NaI(TI) scintillator from Harshaw, 10.4 cm long and 13.0 cm in diameter, viewed by a Philips XP1040 photomultiplier tube. The associated electronics[+], consisting of a pulse-shaping unit and a discriminator, was coupled directly to the photomultiplier tube socket and gave a fast leading-edge time pulse and a linear pulse.

In this series of investigations a NaI scintillator was used for gamma radiation detection due to its high efficiency. As the counting rates are very low it was found to be more important to detect as many events as possible than to get high resolution but low efficiency as with a Ge(Li) detector.

A lead collimator, movable in parallel with the direction of the detected fragments and also with a variable slit, was used to select gamma radiation in different time intervals after the fission event.

The fissile deposit was about 1 cm^2 in area and prepared by electrodeposition on 100 $\mu g/cm^2$ nickel foils. In all runs when mass selection was used the ^{235}U target was less than 100 $\mu g/cm^2$.

It is very important in this type of measurements that the uranium layer and the nickel foil are thin and uniform. The fragment energy loss has not been measured but may be estimated to be $\leq$ 3 MeV [23, 24]. As will be discussed below, the fragment energy spectra were used to get mass spectra, and it was found that an upper practical limit of less than about 100 $\mu g/cm^2$ was enough to get energy spectra of good quality. In some measurements, however, when mass selection was not necessary, or for some reason not possible, thicker layers, of up to about 400 $\mu g/cm^2$, were allowed.

[+] Designed and built at the Research Institute of National Defence, Stockholm [25].

A block diagram of the electronics is shown in fig. 2. Pulses from the solid state detectors were amplified in charge-sensitive preamplifiers followed by linear amplifiers. After delaying one of the pulses and stretching both of them, they were added and fed into a logarithmic amplifier, the output pulse heights of which were proportional to the logarithm of the incoming pulse heights [24, 26]. By disregarding prompt neutron evaporation and energy losses in the target material, it can easily be shown that the ratio of the energies of the two fragments is inversely proportional to the mass ratio.

At an early stage of the experiment a fast coincidence circuit was used, triggering on time pickoff pulses from both fragment detectors, to start the time-to-pulse-height converter (TPHC), so that no timing signal passed unless both fragments from a fission event were registered [24]. Later the fast coincidence circuit was removed and the TPHC was started with pulses from one fission detector. In case only one fragment was detected, i. e. the other fragment missed its detector no mass pulse was recorded. The only problem with this latter arrangement was that for every run the number of measured fission pulses counted on the "timing" fission detector had to be checked and related to the recorded number of mass pulses (when both fragments of an event were detected). With this geometry there is a factor of 1.5 - 2 between these two numbers due to the different solid angles of the fragment detectors.

After amplification the timing pulses were sent into a single channel analyzer (SCA) with its window set over the gamma peak in the time-of-flight spectrum. The output of the SCA then served as the coincidence pulse for the multichannel analyzer.

Data were stored in a two-parameter analyzer the memory of which was

that of a small computer, PDP-8/S. It should be noted that the PDP--8/S was not working as a normal on-line computer, because no data analysis was done during the measurements, but only recording of events. Data analysis was done with separate programs after the measurements were completed [27, 28].

The interfacing unit between the computer and the nuclear physics electronics consisted of two ADC's and their associate registers. Each ADC had 400 channels and the computer memory consisted of 4 K words, i.e. 4096 positions or channels. When an analysing signal had passed its ADC,(or in a two-parameter mode two signals had passed their respective ADC's) it was stored momentarily in its respective register, from where the computer transferred the information into the memory. Of the 4096 channels in the computer memory 3200 channels could be used for data storage. The rest of the memory was used for programs performing operations such as transfer of data into the memory from the nuclear physics electronics, for display on a CRT, and for readout on a typewriter and/or a punch. The 3200 channels could then be divided into matrices of the following forms when measuring with two parameters: 8 x 400, 16 x 200, 32 x 100, or 64 x 50. In a one-parameter mode any of the above-mentioned single configurations was available.

The NaI detector was placed about 70 cm from the fission foil and in a direction perpendicular to the direction of the detected fragments (fig. 1). The main reason for using the time-of-flight technique was to discriminate the prompt neutrons from the fission gamma radiation, but in this geometry it was possible to benefit by the form of the angular distribution of the prompt neutrons. As is well known,it is peaked in the direction of the fragments.

It might be mentioned at this point that a change of distance between the fission foil and the gamma detector did not change the solid angle for gamma detection according to the inverse square law, as would be expected, but instead almost linearly. This is due to the fact that the gamma collimator is mostly set with a narrow slit and the change in solid angle with distance is almost completely dependent on the length of the collimator. Solid angles of the order of 10^{-4} - 10^{-3} sr are normal in these measurements, but, as will be discussed in a coming report [29], this small solid angle is primarily dependent on the collimator setting and not so much on the distance between the foil and the gamma detector.

2.2. Performance

A typical mass spectrum from the thermal fission of ^{235}U recorded with the logarithmic amplifier is shown in fig. 3. The relative yield of fragments in a particular mass region is, of course, not the same as it is when the mass spectrum is on a linear scale. This is a drawback when comparisons are to be made with various relative yields as functions of fragment mass and the other results have been obtained with the fragment mass on a linear scale. Direct quantitative comparisons cannot be made, though it is possible to calculate a new yield curve as a function of mass on a linear scale. The variation in the energy of the prompt photons with fragment mass is, however, a very slow function, and so part of the drawback will be less important in this experiment as one is allowed to consider these photon yields as functions of mass regions instead of individual masses [1]. In any case qualitative comparisons can be made.

Some typical time-of-flight spectra are shown in fig. 4 and 5. Fig. 4 shows a spectrum of the uncollimated gamma radiation with no gamma-ray energy discrimination. The gamma detector was "viewing" the whole region between and including the two fragment detectors. The general background which has no correlation to the fission events is the level to the left of the gamma peak, and the broad distribution just to the right is the prompt neutron yield. The time separation at the NaI detector between the fission gamma radiation and the prompt neutrons of largest yield is about 30 ns, which is achieved for a time-of-flight distance of about 70 cm. In fig. 5 are plotted time-of-flight spectra with the lead collimator in three different positions, which means that only small parts of the fragments' paths are "seen" by the gamma detector.

As indicated in fig. 4 the full width at half maximum (FWHM) value of the gamma peak is 5 ns. This is due to three basic causes: 1) time walk due to amplitude variations in the detector signal, 2) different velocities of the fragments giving a spread in the arrival time at the detector, and 3) the resolution of the gamma timing circuit. Time spectra were measured for coincident fission fragments by causing the TPHC to be started by the signal from one fragment detector and stopped by the signal from the other, resulting in two-peaked curves of the type shown in fig. 6, having a FWHM value of 3.7 ns. The FWHM value for each detector can thus be estimated to be a little less than 2 ns. The time spread in the gamma timing circuit is about 4 ns [25].

The question is whether any improvements can be achieved or not in the FWHM value of the gamma peak in the time-of-flight spectra. This is important to know, because a "narrower" gamma peak is an improvement on the signal to background condition in the gamma energy spectra. One approach would be to put the "time detector" as close as possible to the fission foil. That would give a reduction of the

interval of the time of arrival of the fragments. But the TPHC would start more often and consequently let through more background pulses. This can be circumvented by means of an extra coincidence requirement, e. g. by letting the time signal arrive in coincidence with a pulse from the other fission detector. The drawback is, however, that the time resolution of the gamma collimator will be worse, because gamma radiation from fragments in a larger solid angle than with the present geometry will be analyzed.

If, for any reason, it is considered to be important to have the "time detector" very close to the fission foil, the other detector could be put further away from the foil and then about the same geometry as now would be used. But in both these cases the "time detector" must be put very close to the foil, which would mean that the detector would be partly in the neutron beam. This is not acceptable, because in the vicinity of the foil, where the fission gamma radiation is mostly studied, there should not be any extra material to give rise to more background. Besides, it is better for the detector itself to be clear of the neutron beam to reduce radiation damage to it.

In a future version of this set-up there are possible improvements to be made in the time resolution, e. g. by use of anti-walk circuits [30]. A factor of two or more may be possible. These improvements were not found to be very important at this stage of the experiment, and so they were not tried.

With the help of the collimator, to select gamma radiation from different time intervals after the fission event, time-of-flight spectra were recorded with the collimator in different positions. The average velocity of the fragments is known to be about 1 cm/ns. By estimating the in-

tensity of the gamma peak the intensity variation with the collimator setting was obtained, i. e. the variation with time after fission.

Of extreme importance is the knowledge of the drift in the electronics. Many of the results given in this report are of the kind: relative yield per fragment mass. To be able to make comparisons between photon yields from all fragment masses, the photon yield from a certain mass is divided by the yield of that particular mass. Accordingly two functions are used, the photon yield as a function of mass and the mass yield curve, and the first function is divided by the second, point by point. The two functions, especially the mass yield function, are steep for very asymmetric and symmetric fissions. Consequently it is very important that the change in position of the respective curves should be as small as possible during a measurement period. Frequent checks of the mass yield curve were made during the measurements. The drift in the mass channel was found to be less than 1 % during a period of two weeks.

All measurements have been made in the coincidence mode, even accumulation of single spectra such as calibrations of fragment mass and gamma-ray energies. The reason for this is twofold. First, the data recording system needed a coincidence (opening) signal for each pulse to be analyzed. This coincidence pulse was obtained from the timing circuit. With the TPHC[+] used in this experiment there is always an output pulse as soon as a start pulse (fission pulse) has arrived. In case no stop pulse has arrived within the range of time set on the converter, the output pulse is derived from the automatic reset of the TPHC. The second reason for using the coincidence technique, which is often more

[+] Type 263, purchased from ORTEC, Oak Ridge, Tenn., USA.

important than the first one, was that quite often comparisons had to be made between coincidence (gated) and single spectra. In order to avoid uncertainties in the pulse heights brought about by different measuring modes, all spectra were recorded in the coincidence mode. As discussed above, yields as functions of fragment mass were compared, and yield functions were also divided by one another, and by making all experiments in the same way one possible source of error was avoided.

As noted, the results are given as functions of fragment groups and not of individual masses. For physical reasons this is acceptable, because, as was discussed by Johansson [1], the character of the prompt gamma radiation varies slowly with mass number. This is fortunate because one cannot study individual fragments with the present type of apparatus. Even if it were possible to select a single mass, one still has to account for charge dispersion. The best mass resolution which can be achieved in an experiment of this kind is a FWHM value of about 5 mass units, which mainly depends on prompt neutron emission, the mass defect of the solid state detectors and the energy losses in the fissile foil and its backing [1, 7]. No thorough investigation of the mass resolution has been made in this experiment, but results from earlier studies of that kind have been published elsewhere together with a detailed description of the experimental equipment [24].

3. RESULTS

3.1. General

The main object of the work presented in this report was to examine the number of prompt photons of different gamma energy portions as

functions of fragment mass. All the investigations have been performed in a time interval of about 10^{-11} - 10^{-9}s. In an integral measurement, the result of which forms the basis for most of the discussion in the following section, a mass spectrum was accumulated in coincidence with fission gamma-rays, by taking the coincidence signal from the "timing" SCA as mentioned in section 2.1. The resulting mass spectrum was in coincidence with all fission gammas irrespective of their energies. Another, more or less preliminary investigation was a two-parameter measurement in which mass was one parameter and gamma-ray energy the other. For each mass it was possible to add the number of pulses in parts of the respective gamma-ray energy spectra, giving the total number of gamma-rays emitted, but now in different energy portions.

3.2. Mass-dependent yield of prompt photons of all energies

The above-mentioned integral measurement started with the accumulation of a direct mass spectrum and after division of the gated mass spectrum by this direct spectrum, the relative number of photons per fragment mass was obtained, and the result in the form of a gamma-ray yield curve is shown in fig. 7. The time interval analyzed here is about 10^{-11} - 10^{-10}s, corresponding to the gamma decays at practically the first mm of a fragment's flight path. The first striking feature of the curve in fig. 7 is the similarity with the so-called saw-tooth curve which is obtained in the study of the prompt neutron yield per fragment mass. Such curves have also been found in earlier fission gamma radiation studies of ^{252}Cf [1] and ^{235}U [11]. In the uranium experiment [11] the errors were rather large, due to difficulties in

determining the exact number of fission gamma pulses over background. A more recent result [19] also showed the saw-tooth character even though the mass resolution was of poorer quality. The general background in the present experiment as estimated from its level in the time-of-flight spectrum (section 2.2) was less then 10 % of the intensity under the gamma peak.

One notices two kinds of deviations from the general appearance of the saw-tooth curve. The first is characterized by the dips at mass numbers 88 and 102. The second is the relatively low yield for both the very lightest and the very heaviest fragments, if they also were to give yields according to a curve of the saw-tooth type, like most of the other fragments do. The curve also seems to have a plateau around mass number 145, i.e. in the so-called transition region.

In some mass regions this yield curve is difficult to compare with the other similar curves [1, 11], e.g. in the regions of closed nucleon shells around mass numbers 132 and 82. The main difficulty in making comparisons with other experiments lies in the fact that these mass spectra are on a logarithmic scale[+]. The fragment mass of 82 is hardly seen in ^{252}Cf fission, but on the other hand there is a relatively high yield of fragments up to a mass number of about 115 in the light mass group, and these fragments have very low yields in uranium fission.

[+] In the course of preparing this report a linear divider circuit has become available for the experiment, so now it is possible to make direct comparisons between results from these studies and those of other fission laboratories. Furthermore it has also become possible in these studies to compare yields in terms of numbers from different fragment mass regions of particular interest, such as mass numbers 132 and 82.

3.3. Mass-dependent yield of prompt photons of specific energies

As mentioned above measurements have also started with the aim of looking at the gamma radiation for different energy portions. These studies will continue and only one preliminary result will be given here. The measurements were made with full use of all circuits shown in the block diagram in fig. 2. As soon as there was a gamma pulse in the time-of-flight spectrum, the "timing" SCA opened the ADC's of the two-parameter multichannel analyzer, to let in for analysis the linear pulses from the mass circuit and the gamma-ray energy amplifier. The data were then stored in a matrix, of the kind described in section 2.1, in the computer memory and were thus available in the form of two-parameter spectra, e.g. gamma-ray energy spectra as functions of fragment mass. In each gamma spectrum it was possible to add up the number of pulses in different gamma-ray energy portions, and by doing so for the various gamma spectra, i.e. for the spectra obtained by the different fragment mass groups, the yield of gammas of a particular energy portion was obtained for the respective mass groups. Dividing these yields by the yields of the mass groups, the latter given by a direct measurement of the mass distribution, resulted in a relative gamma-ray yield as a function of fragment mass. Two examples of such yield distributions are shown in fig. 8, which also indicates the respective gamma-ray energy portions for which these functions have been calculated. The lower part of the figure presents the relative gamma-ray yield as a function of mass for photons of energies less than 0.33 MeV, and the shape of the curve is roughly of the saw-tooth type. When photons of energies above 0.33 MeV but less than 1.35 MeV are studied, the yield function is not at all of the saw-tooth type. The time range studied here is from about 0.4 to 1 ns.

3.4. Time distribution

The half-life of one fission gamma component has been estimated by recording time-of-flight spectra with the lead collimator in different positions. The intensity variation of the gamma peak with the collimator setting gave the same variation with time after fission and in a decay curve of the same shape as shown in ref. 1 the half-life was estimated to be about 20 ps. The studies of the time distribution of the gamma radiation have been continued with a more sophisticated collimator system than was used in the present experiment, and those results will be published elsewhere [29].

3.5. Gamma-ray energy spectrum

In fig. 9 is shown a gamma-ray energy spectrum of all prompt fission gammas. It was recorded in coincidence with the gammas of a time-of-flight spectrum of the same type as shown in fig. 4. The overall background is very low, namely less than 1 %. No corrections have been made for the response function of the detector. The shape of the spectrum is the same as those recorded earlier by, e. g., Maienschein [31].

4. DISCUSSION

4.1. General

The observed fine structure of the relative gamma-ray yield as a function of fragment mass can be described in terms of the collimator definition, i. e. it is caused by geometrical effects of the collimator, which for each setting selects photons from a certain time interval and in which the gamma decay rates differ from one fragment mass region to another. Fragments which are slow gamma emitters compared

to the time associated with the collimator setting and fragment velocity will give rise to dips, as will also fragments which are fast emitters. The former fragments have emitted few gamma quantas when they have just passed the collimator opening and the latter fragments have emitted a larger number even before they pass the collimator. A certain half-life will be dominant at a particular collimator setting and other half-lives will be suppressed. This feature of fast and slow gamma emitters is, of course, directly related to the properties of the fragment masses and their excitations. Deformed nuclei seem to be slow fission gamma emitters [2, 29], e.g. in a time interval after scission, when a 50 ps half-life is selected, there is a large intensity of low energy photons, with energies of about 200 keV, emitted by fragments with mass numbers around 110 and above 150.

A complete analysis of the gamma-ray yield curve in fig. 7 must include the following properties and their interrelations: the distributions of time of the fission gamma radiation, of the photon energy, and of the fragment mass. The yield curve in fig. 7, however, reflects, the integrated number of photons in a specific time region after fission as a function of mass. The reason for showing just this curve is its association with a time region which is very interesting as far as the prompt gamma radiation is concerned. As was discussed in ref. 1, during the first 25 ps or so the fragments emit photons of rather equal energy. This is an important consideration because, if it were not so, to mention the number of photons would have no meaning at all. The number of photons times their energy corresponds to the total amount of energy released by the gamma decay, and that is the quantity which is of ultimate interest in this fission study. As will be discussed later [29] the yield of photons of different gamma-ray energy varies with time after fission and thus

the collimator setting is a parameter of great importance.

The number of photons and their energies is worth some extra attention before discussing the details of the yield curves in fig. 7 and 8. As was pointed out in section 3, the yield curve in fig. 7 looks similar to the well-known curve of the saw-tooth type representing the yield of prompt neutrons as a function of fragment mass. The gross appearance of the curve is about the same for both cases. In many respects the present discussion will run along the same lines as that when studying the yield of prompt neutrons per fragment mass. The prompt neutron yield curve does not show up so many details as this gamma-ray yield curve. The absence of this structure in the neutron yield curve as compared with the gamma-ray yield curve is probably due to the fact that the neutron yield concerns all neutrons, while the gamma yield concerns the number of photons emitted in a relatively short time interval. Consequently it can be expected that most of the "unusual" effects discussed here will disappear if the relative number of photons as a function of fragment mass is studied in a time interval which is longer than that for which fig. 7 is valid, namely 10^{-11} - 10^{-10} s.

So far very little attention has been paid to the mass-dependent structure of the gamma-ray yield function and its association with time after fission. Short mention of it was made by Johansson [1, 2], but to our knowledge only brief investigations have been made [32 - 35].

4.2. Mass-dependent yield of prompt photons of all energies

The discussion will now deal with the yield of the prompt gamma-rays as a function of fragment mass (fig. 7) from the point of view of nuclear structure, and specifically in terms of spherical and non-spherical nuclei.

One of the assumptions in fission theory is that most of the original excitation energy of the fragments, directly after the scission act, is taken up by deformation [36]. In this respect every fission mode must be considered by studying the joint contribution from the fragment pair. The shape of the nuclei as described by the shell theory or the collective model, whenever any of them fits into the description, can be applied in the following way. A spherical nucleus, with one or both nucleon shells almost closed, is resistant to deformation, and its excitation energy directly after fission should not be so high as in a nucleus which can easily be deformed, i. e. one or both of its nucleon numbers are far from magic. If the excitation energy of certain fragments is high, due to the fact that they are easily deformable (soft fragments), they are able to emit more neutrons and photons than fragments which are not easily deformable (stiff fragments), because in the latter one or both nucleon shells are closed or almost closed. A full discussion of this problem has been given by Vandenbosch and Terrell [37, 38]. The sawtooth curve reflecting the yield of the prompt neutrons as a function of fragment mass is well described by this picture. Take one example, e. g. the binary fission of ^{236}U into the fragment pair with mass numbers 110 and 126. The light fragment will probably have the proton number Z = 44 and the neutron number N = 66, and the heavy partner will then have the respective nucleon numbers Z = 48 and N = 78. The heavy fragment is rather stiff, while the light fragment is more soft. The prompt neutron yield for fragments in the mass region around 110 is much larger than around 126. The whole prompt neutron yield curve can then be discussed in the same way as in this particular example. Further sup-

port for this model is given by the application of a so-called "universal" yield curve [36]. The absolute number of prompt neutrons from a particular fragment is about the same, no matter in which fission process it was formed. A "universal" saw-tooth type curve is the result of prompt neutron yields known so far in low-energy fission, from fissile nuclei with mass numbers all the way from thermal neutron induced fission of ^{233}U to spontaneous fission of ^{252}Cf.

The description given here of the excitation of the fission fragments and their consequences on the prompt neutron decay can be borrowed to discuss the prompt gamma decay following neutron emission. In principle the discussion is the same, but, as was pointed out above, one must never forget that the photon energy should be included. The fission gamma radiation of shortest half-life, which can be selected with the available collimator without making it too narrow for intensity reasons [29], seems to have about the same energy for all fragments. The yield curve looks similar to the prompt neutron yield curve, because the fragments are still highly excited after the neutron emission, the excitations being higher the higher the original excitations have been. As has been pointed out by Johansson [1], one might expect that at the first moment the fragments emit a similar type of radiation, and the basic reason for this is that all fragments are probably deformed in a similar manner, giving rise to neutron emission because the excitations are high enough, and then prompt gamma emission of similar type over the whole mass spectrum.

On the basis of the above-mentioned model, in which the rigidity of the fragments is an important quantity, the discussion will now turn to a direct application of that model. In order to see things more clear-

ly, a figure is drawn to explain the locations of the fission fragments on an isotope chart. Fig. 10 shows the part of the chart of particular interest in this investigation. The line of beta stability is drawn as a solid curve and the light fragment group in uranium fission is represented by the dashed line. The mass regions for which low gamma-ray yields have been observed, as presented in fig. 7, are shaded in fig. 10. One such portion is around mass number 82 where the neutron number is expected to be about 50, another around 88 where the two nucleon shells may start to be deformed and a third portion is around 102 where the proton number is about 40.

When the mass number increases from 82 and upwards one would anticipate effects in the yield curve in fig. 7 which may be due to the deformation of those nuclei. Such effects would set in at mass numbers around 88, and then last through the rest of the light part of the mass curve as, according to the shell theory, there is no other closed nucleon shell than N = 50 in the mass region where the light mass group is located. A change of yield takes place, however, around the mass number 96, and the gamma-ray yield curve has there come up to values corresponding to an average saw-tooth type curve drawn through most of the values plotted in the figure. The presence of the two dips at mass numbers 88 and 102 may indicate the existence of variations in the deformation of nuclei in these mass regions. Z = 40 should be the proton number for fragments of mass number around 102. The relevant neutron number for A = 102 is N = 62. The proton shell is almost spherical, but the neutron shell with 12 neutrons outside the closed shell of N = 50 might be easily deformable.

Under the condition that the fragments with mass numbers around

102 have nucleon shells, $Z \approx 40$ and $N \approx 62$, it may be interesting to study available data on level schemes from nuclei in their vicinity on the nuclide chart. Take, for instance, the fragments with mass numbers around 102. The proton number is expected to be about 40, and the neutron number to be about 62. This neutron-rich mass region is not easily accessible with today's accelerator technique. The line of beta-stability (fig. 10) goes through $Z = 40$ and $N = 50$. These stable nuclei have few excited levels at low energies, which is explained by the shell theory as being due to the resistivity of closed shells to excitation of one or two nucleons. The neutron number is 50 and magic, but the proton number of 40 can, according to the shell theory, be called a semi-magic number. The presence of this semi-magic number may indicate the difficulties which will be encountered when one tries to extrapolate the energies of certain types of excited states of nuclei at the beta-stability line into the regions where these fragments have been formed. Another example is the fragment mass region around $A = 88$ with $Z = 34$ and $N = 54$. If one tries to extrapolate the energies of certain types of levels in different isotopes of selenium, one soon approaches $N = 50$ where the energies of the excited levels go up due to the fact that one approaches a closed neutron shell. Instead the extrapolation can start with fixed neutron number, say $N = 54$. Very soon one sees effects setting in close to $Z = 40$, and then there are few data available when Z is less than 40 and N still 54. Of particular interest is the fact that the sister fragment to 102 is 134, which is close to being double-magic ($Z \approx 51$, $N \approx 83$). Without being able to give any exact numbers for comparison, the relative yield, as seen in fig. 7, is larger from the fragment with mass num-

ber 102 than it is from 134. This particular fission mode consists of a spherical nucleus, A = 134, which is thus stiff. As regards the partner fragment with A = 102 its yield of both prompt neutrons and prompt gamma radiation is larger than that from the fragment with A = 134.

The mass region around A = 110 deserves some extra attention, because the fission gamma studies in ^{252}Cf fission have given rather strong evidence that this mass region may have stable deformation [2, 39]. In the ^{252}Cf gamma-ray yield curve there is a dip in this mass region with about the same collimator setting as was used in the present experiment. Unfortunately the fragment yield in the mass region around 110 is very low in ^{235}U fission, while in ^{252}Cf fission the same mass region is almost where the fragment yield is the largest in the light mass group. Even though it may be difficult to make any detailed comparisons between the two yield curves in this mass region, some interesting and differing features occur. In the ^{235}U fission there is an anomalously high gamma-ray yield, contrary to the case in ^{252}Cf fission. This difference can probably be explained by studying the two fission modes in ^{235}U and ^{252}Cf fission resulting in a light fragment with mass number around 110. The sister fragment in ^{235}U fission has a mass number of 126, which means that it must be almost spherical (Z = 48, N = 78), while in ^{252}Cf fission the number is 142 which probably corresponds to a nucleus which is slightly more susceptible to deformation. This is because this mass region is close to the so-called transition region. Under the condition that quantities like energy and linear momentum are conserved in the fission process, it is very instructive to study the respective combinations of fragments in binary fission under these cirumstances. If a certain fission mode results in

one spherical (stiff) fragment and one fragment with both nucleon numbers somewhere between the magic numbers 50 and 82 (soft fragment), the soft fragment will be able to tie up more deformation energy than the stiff fragment. ^{252}Cf symmetric fission results in the two stiff fragments with A = 126, while in ^{235}U fission, resulting in fragments with A = 126 and 110, most of the deformation energy is imparted to the fragment with A = 110. In ^{235}U fission one must expect to have relatively more excitation energy in the fragment with mass number 110 than the same fragment would have if it was formed in ^{252}Cf fission.

When the gamma-ray yield from the fragment mass region of 102 was discussed, it was seen in fig. 7, that the partner fragment with mass number 134 had a lower yield than 102. The heavy fragment emits a smaller number of photons and from this reasoning one can only conclude that the light partner is relatively soft compared to the heavy one. So-called deformation parameters characterizing the resistivity of the fragments to deformation have been calculated [38] and they have their largest values for N = 50, Z = 50, and N = 82, but there is a slightly larger value for Z = 40 than would be expected if Z = 40 was not a semi-magic number. It must be mentioned that these deformation parameters were calculated directly from fission data, and not through the use of extrapolations.

Now it is easy to complete the discussion of the appearance of the gamma-ray yield curve in fig. 7 with the fragment structure in mind. With increasing mass number the prompt neutron yield curve falls off sharply when the region of symmetric fission is reached. The gamma-ray yield curve in fig. 7 does the same, which is in agreement with the discussion above.

The relatively low yield in the mass region around A = 132 has already been discussed in relation to the partner fragments. The plateau around mass number 145, which is where the transition region is reached, is difficult to explain. It is a bit too low in mass number to be the partner fragment of 88, where another of the dips in fig. 7 occurred, and which could be due to some susceptibility to deformation. The probability that the dip at A = 88 and the plateau at A = 145 are due to a specific fragment combination cannot be completely ruled out at this stage, because if the mass calibration is changed by one unit downwards around A = 88 and A = 145, one is close to the fragment combination which would fit into this picture. The prompt neutron release may also contribute to give the proper mass around A = 145. The plateau at A = 145 can consequently be due to the fact that the light partner fragment is slightly soft and therefore able to pick up some extra deformation energy which will be obtained at the expense of the excitation of the heavy partner.

Finally the decrease of the prompt gamma-ray yield as a function of fragment mass in fig. 7 when the mass exceeds 148 should be mentioned. This is probably most obvious on the basis of the models used so far in this paper. The fragments with mass numbers above 148 are deformed and belong to the same mass region where many other deformed nuclei have been found.

4.3. Comparisons between prompt photon yields in ^{235}U and ^{252}Cf fission

In order to try further to illuminate the situation regarding the fission-fragment gamma-decay in ^{235}U fission, it is interesting to make

comparisons with some of the known data from prompt gamma radiation in ^{252}Cf fission. The yields of the K X-rays and the conversion electrons as functions of fragment mass are both strongly increasing functions in the heavy mass region [4, 6-9, 12, 14, 16], until mass numbers around 148 are reached, when the yields suddenly drop. There have been discussions in the literature about this effect, and even though most authors seem to believe that it is a physical one, arguments have been put forward as to its origin. Whatever the reason is for this drop of yield, in some measurements it was found to be less drastic when the studied time region after fission was longer. This maybe due to the fact that many of the converted transitions come from rather long-lived states with life-times of the order of some tens of ns. Comparisons between the K X-ray and conversion electron yield curves as functions of fragment mass with that of the delayed gamma radiation in ^{252}Cf fission [2] may support this assumption. Around the mass number A = 155 a large yield of photons was found. This fits well into the description given at the beginning of this section, according to which it is expected that most of the "unusual" effects showing up in fig. 7 will disappear when longer time intervals are studied. This statement was made in connection with the prompt neutron yield discussion and has now found further support.

Some arguments have been advanced [8, 9, 12, 41] concerning the relatively low K X-ray and conversion electron yield in the heaviest fragment mass region. The energies of the first excited states of these fragments are believed to be so low that a proportionally small number of electrons are converted [41]. This is a plausible result, which cannot be tested further for the time being owing to the absence of this type of information from fission fragments or similar nuclei.

As was mentioned above, when the relatively low yield of prompt photons from fragments with mass numbers above 148 was discussed (fig. 7), comparisons made with delayed gamma radiation in ^{252}Cf fission [2] favoured the argument that, both in ^{235}U and ^{252}Cf fission, the heaviest fragments are slow gamma emitters. The mass region around A = 110 is interesting from this point of view. In ^{252}Cf fission [2] a large yield of delayed gamma radiation was found there too. On the assumption that deformable fragments are slow emitters, the dip in the relative gamma-ray yield curve as a function of fragment mass for prompt gamma radiation in ^{252}Cf fission corresponds to the increased yield in the same mass region for delayed radiation. The question is how can this increased yield correspond to the same fragments having a large yield of prompt photons in ^{235}U fission. As mentioned earlier, it is probably an effect associated with the particular fission mode in uranium, where the fragment with mass number 110 has a partner with mass number 126, the latter being very stiff, and thus most of the excitation energy, in the form of deformation just after scission, is imparted to the lighter fragment. In californium fission the heavy partner of the fragment with mass number 110 is 142, which is probably more deformable than 126.

The other mass regions in ^{252}Cf fission giving large yields of delayed gamma radiation are 92, 96 and 132 [2]. The delayed radiation emitted by fragments of mass numbers around 132 was thought to be caused by vibrations in the double-magic nuclei, in which the gamma transitions from the third to the second, and from the second to the first excited state in a beta-vibration cascade have energies in the range of 100 - 300 keV, and are thus rather slow. The ground-state transition

energy is expected to be something between 1 and 1.5 MeV. Indications of all these transitions showed up in the gamma-ray energy spectra for the delayed gamma transitions in ^{252}Cf fission. The large yield of delayed gamma radiation in ^{252}Cf fission in the fragment mass regions around 92 and 96 seems to have no correspondence in the present ^{235}U data. Nor need it have, as the two fission processes result in unequal modes. Both fragments are in a region about five units or more from the magic numbers, A = 92 corresponds to Z = 36, N = 56 and A = = 96 corresponds to Z = 38 and N = 58. In ^{252}Cf fission both fragments have partners in the deformed mass region, as the partner of 92 is 160 and of 96 is 156. The respective partners in ^{235}U fission are 144 and 140. On the same basis as before, that in a particular fission mode the softest fragment ties up most of the available deformation energy, it can only be concluded that the light fragments are less excited in ^{252}Cf fission than in ^{235}U fission.

Unfortunately there is no result of the delayed gamma-ray yield in ^{235}U fission of similar accuracy to that in ^{252}Cf fission [2] to make a detailed comparison between the yield curves. A direct comparison is, however, very difficult between yields of prompt and delayed phottons. The first part of the prompt gamma decay seems to take place in a similar way in the case of all fragments as far as the energy is concerned, and the number of photons can help to get a rough estimate of the original excitation of the fragments. As discussed in ref. 1, this is probably due to the fact that the fragments, as they are formed in a scission act, are probably all of them deformed in a similar way. The soft fragments can take a relatively long time to come down to their ground states. They have more deformation energy than the stiff nuclei if a pair of these

two types of fragments have been formed in a scission act. The spherical nuclei may also be slow gamma emitters, as discussed above. Their deformations, however, are normally less than those of soft fragments, causing less excitation energy. It is here, after the first decays, that one must start to consider the energy of the photons, when direct comparisons between the gamma-ray yield curves become more or less irrelevant, at least if one tries to compare numbers. One example will show this. The gamma-ray energy spectra [29] show a very large yield of photons of energies around 200 keV in the mass regions around 110 and above 148. The half-life of the integral gamma radiation is about 50 ps. The low yield for fragments with mass numbers above 148 will increase if the yield curves from a prompt and a slow gamma decay are added. In the same time region in which the gamma radiation with the 50 ps half-life was enhanced, there was an increased yield of photons of energies around 1.2 MeV and 250 keV from fragments in the mass region around 132. It does not make sense to add up numbers of photons of such different energies and then compare with numbers obtained from other kind of spectra. The crucial quantity from the beginning of the gamma decay is the total excitation energy which is obtained through the fission act, even though in this experiment it is studied after the prompt neutrons have been released.

4.4. Mass-dependent yield of prompt photons of specific energies

The gamma-ray yield curves in fig. 8 have not been discussed explicitly so far, but an analysis indicates that the prominent features of those two curves have more or less been considered while discussing fig. 7. The time region studied goes from 4×10^{-10} - 10^{-9}s and

the above-mentioned half-life of 50 ps is enhanced. The lower yield curve shows a large relative yield of photons of energies less than 0.33 MeV from the heaviest fragments in both the light and the heavy mass group. As was mentioned above a later but not yet fully analyzed experiment indicates that both these types of fragments have very large yields of photons of energies around 200 keV. The mass number is on a logarithmic scale, so the yields above the mass numbers 148 will increase relative to the 110 yield if the data are taken with the mass number on a linear scale. The newer data have given yields of 200 keV photons which are about equal in these two mass regions for a certain collimator setting enhancing the gamma radiation of 50 ps half-life. As far as the higher energies are concerned the yield of photons of energies between 0.33 and 1.35 MeV is somewhat larger in some particular mass regions, such as A = 90 and A = 135. In later experiments the division of gamma-ray energy intervals, and also the energy spectra, has shown that there is a relatively large yield of 1.2 MeV photons from fargments with mass numbers around 132, and then also from the very lightest fragments.

5. CONCLUSIONS

In this report a presentation has been given of one way of studying prompt gamma decays from fission fragments. One of the basic ideas behind the experimental set-up, namely that of using a collimator for the separation of the radiation from the two fragments of a fission event, has been applied earlier [1, 2], but the technique has here been developed by the incorporation of time discrimination between the prompt fission gamma radiation and the prompt neutrons. Recently a similar set-up was reported to the IAEA Fission Symposium in Vienna, 1969 [19].

The experiment performed with it was, however, different in most respects from that presented in this report. One of the most important points in the present measurement is the collimator definition and the associated time resolution. It has shown that it is possible to get acceptable signal to background ratios even with rather narrow slits and in a reactor surrounding, where the background is very high.

Fission gamma radiation as such can most successfully be studied in ^{252}Cf fission due to the low background, but complementary data from ^{235}U fission is of great value for several reasons:

1) the light mass group is different in the two types of fission,
2) one wants to know as much as possible about the total energy release of the fragments,
3) details of the fission gamma energy-spectra can be of help in the analysis of the neutron capture gamma-ray spectra to determine background,
4) as a by-product one may be able to study the (n,γf) process, which is of great importance for the knowledge of the fission process.

Some of the difficulties encountered in fission-gamma data analysis have been discussed, and particularly those concerning the extrapolation of energies of certain types of excited states in nuclei at the line of beta-stability when going out to mass regions involving the light fragment group. A fruitful way will be opened in the near future when more and more data have come out of the experiments now in progress at the on-line isotope separators, such as ISOLDE, TRISTAN, OSIRIS and others [42]. A completely new kind of spectroscopy has started, as one now studies neutron-rich nuclei far off the stability line.

Investigations with the present technique have continued and data analysis is in progress. Special emphasis has been laid upon the study of gamma-ray energy spectra as functions of mass, time after fission, and the total kinetic energy of the fragments.

ACKNOWLEDGEMENT

It is a pleasure to thank Prof. S. Johansson and Dr. N. Starfelt for their deep interest, the former for his ideas and patient handling of many of our problems, and the latter for his active and continued support when, as former Head of the Neutron Physics Section of AB Atomenergi, he made this experiment possible. Thanks are also due to Prof. N. Ryde and Dr. T. Wiedling for their interest, the latter in his character of Head of the Neutron Physics Section, and also for his critical review of the manuscript. The authors are grateful to Dr. J. Higbie for his assistance and trouble in getting the electronics to work. One of us (H. A.) is indebted to "Statens råd för atomforskning" for financial support.

REFERENCES

1. JOHANSSON S. A. E.,
Gamma de-excitation of fission fragments.
(I). Prompt radiation.
Nucl. Phys. 60 (1964) p. 378.

2. JOHANSSON S. A. E.,
Gamma de-excitation of fission fragments.
(II). Delayed radiation.
Nucl. Phys. 64 (1965) p. 147.

3. JOHANSSON S. A. E. and KLEINHEINZ P.,
Gamma-radiation from fission.
Alpha-, beta- and gamma-ray spectroscopy.
Ed. by K. Siegbahn. North Holland Publ. Co.
Amsterdam 1965. Vol. 1, p. 805.

4. Physics and chemistry of fission.
Proc. of a symp. Salzburg, 22-26 March 1965.
(IAEA) Vienna, 1965. Vol. 1 and 2. Sess. IV and VII.

5. KAPOOR S. S. and RAMANNA R.,
Emission of prompt gamma rays in the thermal-neutron fission of U^{235}.
Phys. Rev. 133B (1964) p. 598.

6. KAPOOR S. S., BOWMAN H. R. and THOMPSON S. G.,
Emission of K X rays and division of nuclear charge in the spontaneous fission of ^{252}Cf.
Phys. Rev. 140B (1965) p. 1310.

7. WATSON R. L.,
A study of the internal conversion electrons emitted within three nanoseconds after the spontaneous fission of ^{252}Cf. Thesis. 1966.
(UCRL-16798)

8. GLENDENIN L. E. and UNIK J. P.,
Division of nuclear charge deduced from X-ray measurements in the spontaneous fission of ^{252}Cf.
Phys. Rev. 140B (1965) p. 1301.

9. ATNEOSEN R. A. et al.,
X rays and electrons emitted in coincidence with the fission of ^{252}Cf.
Phys. Rev. 148 (1966) p. 1206.

10. VAL'SKII G. V. et al.,
Gamma-ray emission times in fission.
Soviet At. Energy 18 (1965) 279.

11. MAIER-LEIBNITZ H., SCHMITT H. W. and ARMBRUSTER P.,
Average number and energy of gamma-rays emitted as a function of fragment mass in U^{235} thermal-neutron-induced fission.
Physics and chemistry of fission.
Proc. of a symp. Salzburg, 22-26 March 1965.
(IAEA) Vienna, 1965. Vol. 2, p. 143.

12. WATSON R. L., BOWMAN H. R. and THOMPSON S. G.,
K X-ray yields of primary ^{252}Cf fission products.
Phys. Rev. 162 (1967) p. 1169.

13. BRIDWELL, WYMAN E. and WEHRING W.,
Half-lives and yields of X rays from thermal fission of U^{235} and Pu^{239}.
Phys. Rev. 145 (1966) p. 963.

14. DOLCE R., GIBSON W. M. and THOMAS T. D.,
Emission times and yields of K X rays coincident with ^{252}Cf spontaneous fission.
Phys. Rev. 180 (1969) p. 1177.

15. KAPOOR S. S., RAMAMURTHY V. S. and ZAGHLOUL R.,
Yield of K X rays emitted from U^{236} fragments.
Phys. Rev. 177 (1969) p. 1776.

16. Physics and chemistry of fission.
Proc. of a symp. Vienna, 28 July - 1 August 1969.
(IAEA) Vienna, 1969. Sess. F and H.

17. POPEKO L. A. et al.,
Delayed gamma rays from U^{235} fission.
Soviet At. Energy 19 (1965) p. 1082.

18. BLINOV M. V. et al.,
Angular anisotropy of the gamma quanta accompanying U^{235} fission.
Soviet Phys. JETP 16 (1963) p. 1159.

19. ARMBRUSTER P. et al.,
Mass dependence of anisotropy and yield of prompt γ-rays in ^{235}U thermal fission.
Physics and chemistry of fission.
Proc. of a symp. Vienna, 28 July - 1 August 1969.
(IAEA) Vienna, 1969, p. 545.

20. GRAFF G., LAJTAI A. and NAGY L.,
The angular distribution of gamma-rays from the fission of U^{235}.
Physics and chemistry of fission.
Proc. of a symp. Salzburg, 22-26 March 1965.
(IAEA) Vienna, 1965. Vol. 2, p. 163.

21. SKARSVÅG K.,
Delayed gamma-rays from spontaneous fission of ^{252}Cf. (Abstract.)
Physics and chemistry of fission.
Proc. of a symp. Vienna, 28 July - 1 August 1969.
(IAEA) Vienna, 1969, p. 927.

22. VERBINSKI V. V., WEBER H. and SUND R. E.,
Prompt gamma-rays from $^{235}U(n, f)$, $^{239}Pu(n, f)$ and ^{252}Cf(spontaneous fission). (Abstract.)
Physics and chemistry of fission.
Proc. of a symp. Vienna, 28 July - 1 August 1969.
(IAEA) Vienna, 1969, p. 929.

23. BOWMAN H.R. et al.,
Velocity and angular distributions of prompt neutrons from spontaneous fission of Cf^{252}.
Phys. Rev. 126 (1962) p. 2120.

24. HIGBIE J.,
Gamma radiation from fission fragments.
Experimental apparatus - mass spectrum resolution.
AB Atomenergi, Sweden, 1969
(AE-367)

25. BECKMAN L., HANSÉN J. and JANSSON R.,
A fast time-of-flight spectrometer.
Nucl. Instr. Methods 52 (1967) p. 157.

26. HOGG G.R. and LOKAN K.H.,
An analogue ratio circuit for fission fragment mass determination.
Nucl. Instr. Methods 33(1965) p. 319.

27. SJÖLIN P.G., GRANSTRÖM K. and BJÖRKMAN J.,
A two-parameter analyser based on a small computer.
1968, AB Atomenergi, Studsvik, Sweden.
(Internal report AE-SSI-229.)

28. LINDOW L. and ALBINSSON H.,
A program package for a small computer.
1969, AB Atomenergi, Studsvik, Sweden.
(Internal report TPM-FFN-100.)

29. ALBINSSON H. and LINDOW L.,
to be published.

30. SHIRAISHI F. and HOSOE M.,
Energy and time-of-flight correlation experiments with solid-state detectors for mass distribution measurement of ^{235}U fission fragments.
Nucl. Instr. Methods 66(1968) p. 130.

31. MAIENSCHEIN F.C. et al.,
Gamma-rays associated with fission.
U.N. intern. conf. on peaceful uses of atomic energy.
2. Geneva 1958. Proc. Vol. 15, p. 366.
(UN) Geneva, 1958.

32. ALBINSSON H., HIGBIE J. and LINDOW L.,
The prompt gamma radiation from fission fragments.
Nuclear structure: Dubna symp. 1968.
Dubna, 4-11 July, 1968.
(JINR, Dubna publication D-3893)

33. ALBINSSON H. and LINDOW L.,
Gamma radiation from fission products.
In Neutron physics laboratory. Annual progress report.
Ed. by T. Wiedling, October 1, 1967 - September 30, 1968.
AB Atomenergi, Sweden, 1969.
(AE-354) p. 17.

34. ALBINSSON H. and LINDOW L.,
Prompt gamma-rays from thermal neutron-induced fission of ^{235}U.
(Abstract.)
Physics and chemistry of fission.
Proc. of a symp. Vienna, 28 July - 1 August 1969.
(IAEA) Vienna, 1969, p. 930.

35. JOHN W., WESOLOWSKI J. J. and GUY F.,
Mass-dependent structure in the fission γ-ray yields from ^{252}Cf.
Phys. Lett. 30 B (1969) p. 340.

36. TERRELL J.,
Neutron yields from individual fission fragments.
Phys. Rev. 127 (1962) p. 880.

37. VANDENBOSCH R.,
Dependence of fission fragment kinetic energies and neutron yields on nuclear structure.
Nucl. Phys. 46 (1963) p. 129.

38. TERRELL J.,
Prompt neutrons from fission.
Physics and chemistry of fission.
Proc. of a symp. Salzburg, 22-26 March 1965.
(IAEA) Vienna, 1965, Vol. 2, p. 3.

39. JOHANSSON S. A. E.,
New regions of deformed nuclei
Why and how should we investigate nuclides far off the stability line.
Proc. of the international symp. Lysekil, August 21-27, 1966.
Arkiv Fysik 36 (1967) p. 599.

40. GLENDENIN L. E. et al.,
High-resolution studies of K X-ray emission and the distribution of mass and nuclear charge in the thermal-neutron-induced fission of ^{233}U, ^{235}U and ^{239}Pu.
Physics and chemistry of fission.
Proc. of a symp. Vienna, 28 July - 1 August 1969.
(IAEA) Vienna, 1969, p. 781.

41. VANDENBOSCH R.,
Discussion in Physics and chemistry of fission.
Proc. of a symp. Salzburg, 22-26 March 1965.
(IAEA) Vienna, 1965. Vol. 1, p. 399.

42. Why and how should we investigate nuclides far off the stability line.
Proc. of the international symp. Lysekil, August 21-27, 1966.
Arkiv Fysik 36 (1967).

FIGURE CAPTIONS

Fig. 1. Schematic diagram of the experimental arrangement.

Fig. 2. Block diagram of the instrumentation for the measurement of fission gamma radiation.

Fig. 3. Pulse spectrum from the logarithmic amplifier.

Fig. 4. Time-of-flight spectrum for the uncollimated fission gamma radiation.

Fig. 5. Time-of-flight spectra for the collimated fission gamma radiation with three different collimator settings.

Fig. 6. Time spectrum from coincident fission fragments.

Fig. 7. The relative gamma-ray yield as a function of fragment mass.

Fig. 8. The relative gamma-ray yield of two different energy portions as a function of fragment mass for a collimator setting not so close to the fission foil as was the case shown in fig. 7.

Fig. 9. The energy spectrum of the uncollimated gamma-rays emitted within 5×10^{-9} s after the fission event.

Fig. 10. The nuclide chart showing the line of beta stability (full curve) and the area of the light fission fragments (dashed curve). The locations of the dips in fig. 7 are indicated by shaded areas.

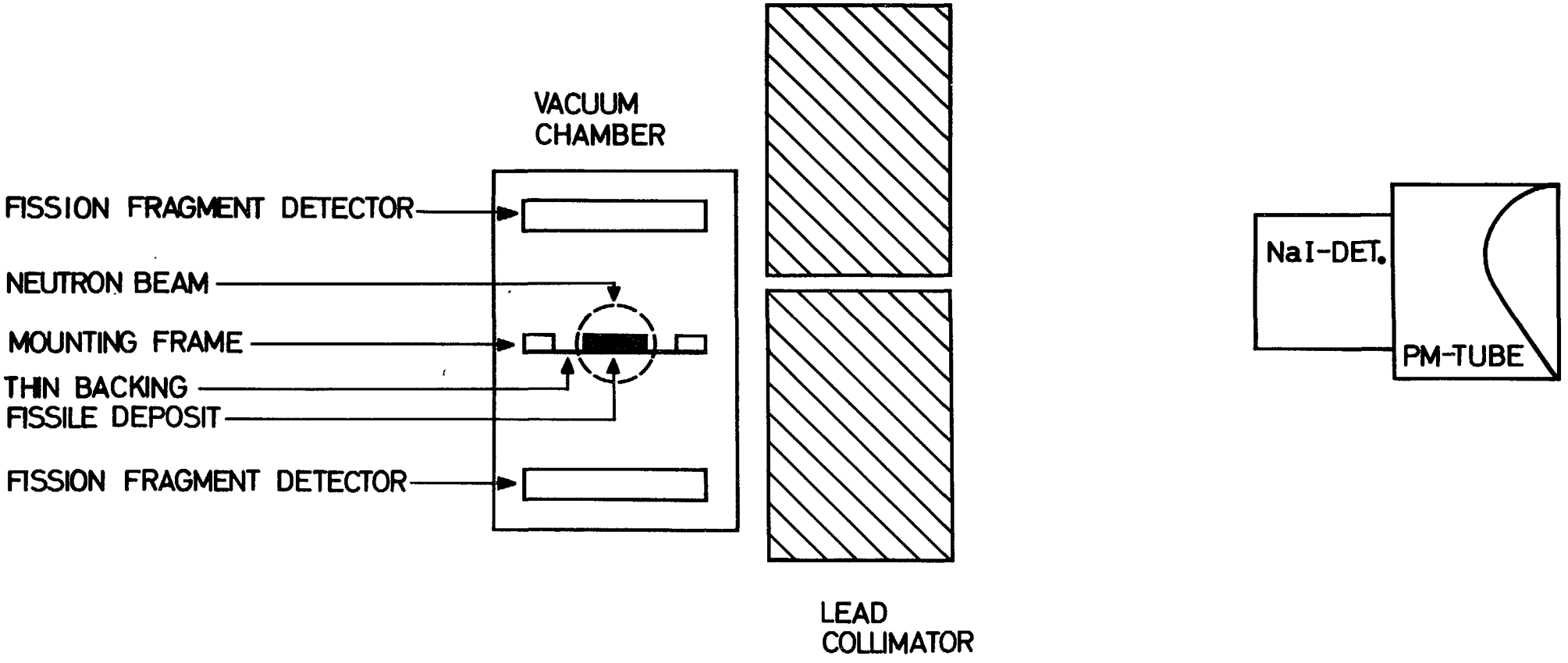
VACUUM
CHAMBER
FISSION FRAGMENT DETECTOR
NEUTRON BEAM
MOUNTING FRAME
THIN BACKING
FISSILE DEPOSIT
FISSION FRAGMENT DETECTOR
LEAD
COLLIMATOR
NaI-DET.
PM-TUBE

Fig. 1

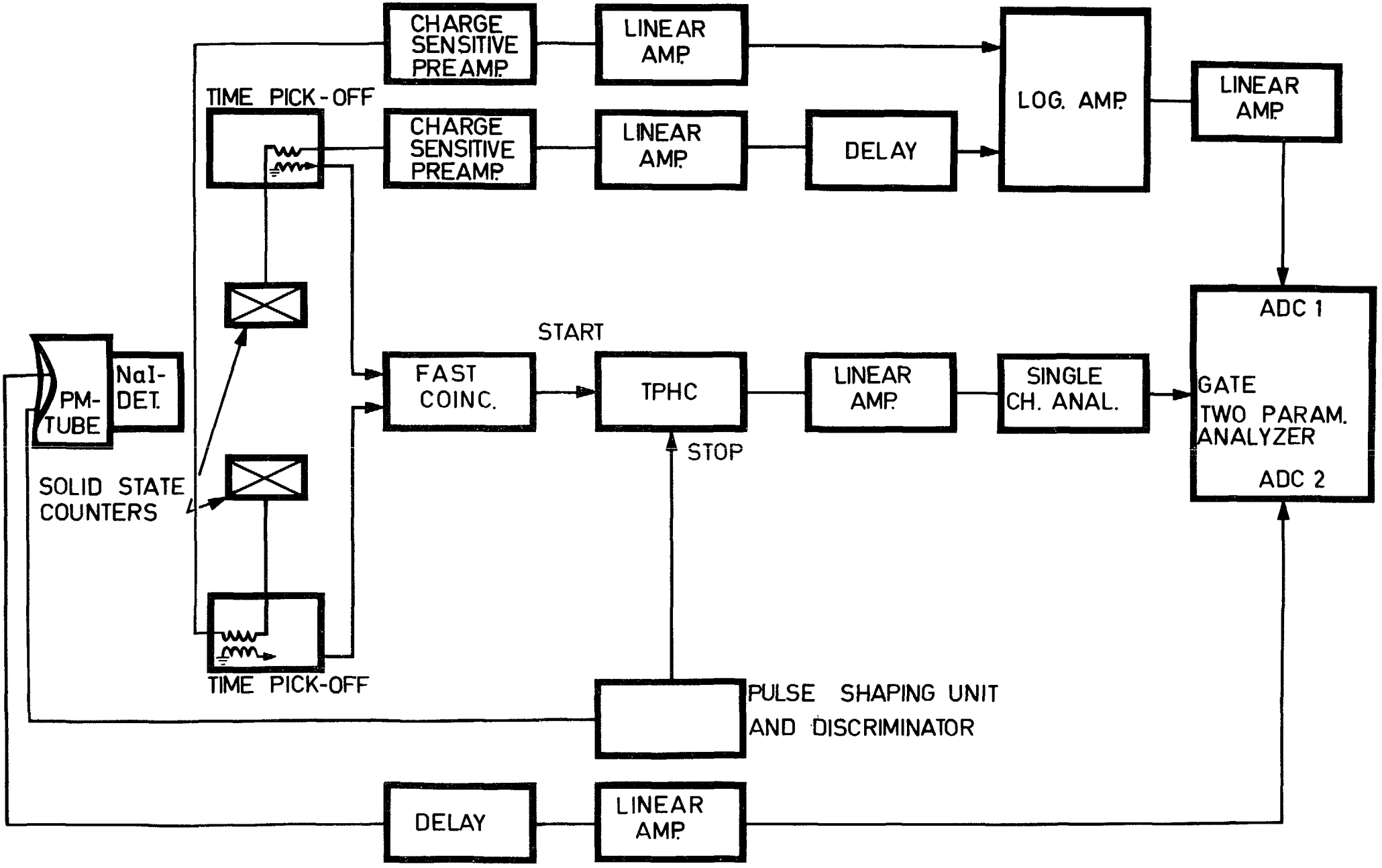
CHARGE SENSITIVE PREAMP.
LINEAR AMP.
LOG. AMP.
LINEAR AMP.
TIME PICK-OFF
CHARGE SENSITIVE PREAMP.
LINEAR AMP.
DELAY
START
ADC 1
NaI-DET.
PM-TUBE
FAST COINC.
TPHC
LINEAR AMP.
SINGLE CH. ANAL.
GATE
TWO PARAM. ANALYZER
ADC 2
STOP
SOLID STATE COUNTERS
TIME PICK-OFF
PULSE SHAPING UNIT AND DISCRIMINATOR
DELAY
LINEAR AMP.

Fig. 2

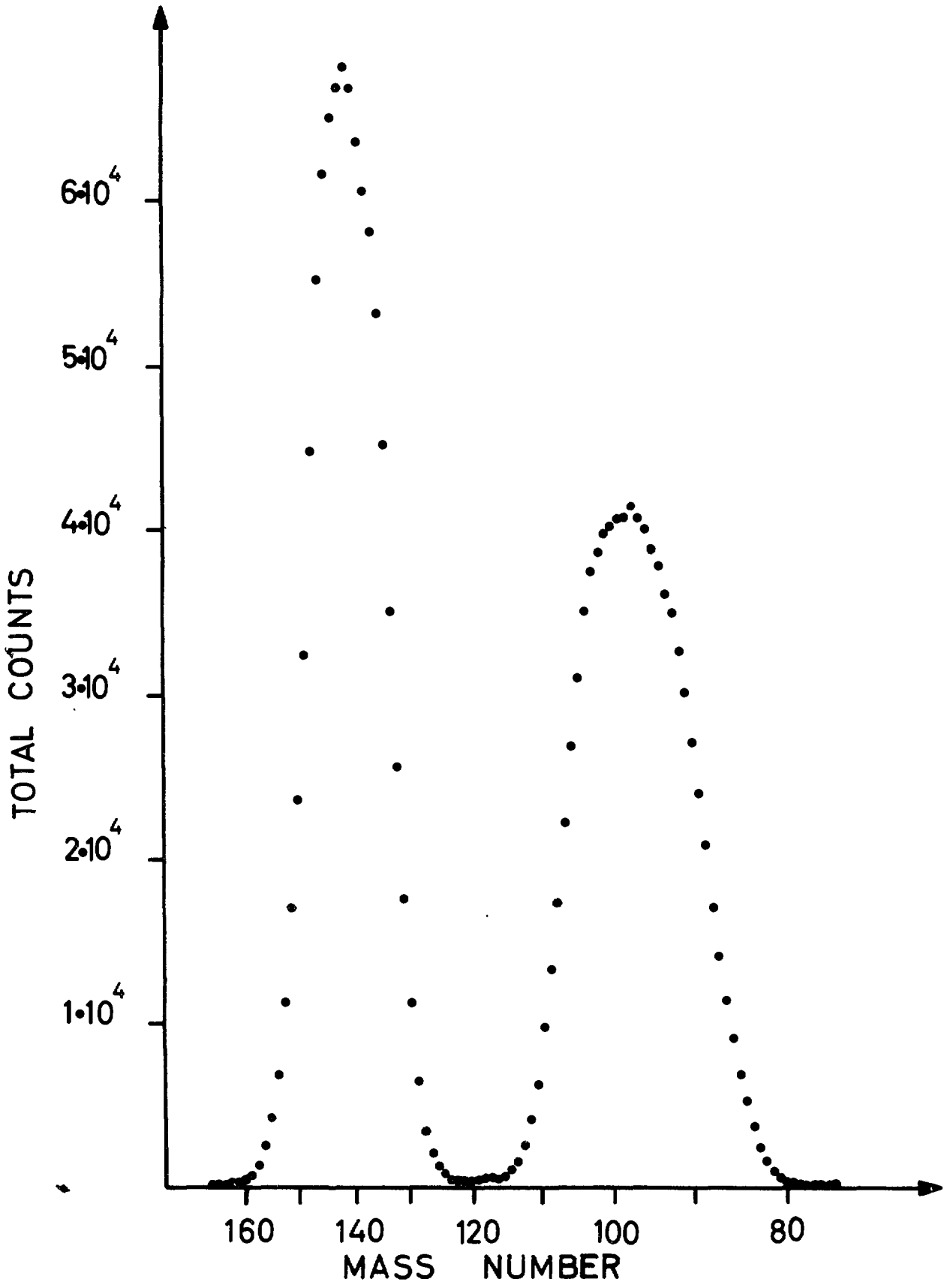
TOTAL COUNTS
6·10^4
5·10^4
4·10^4
3·10^4
2·10^4
1·10^4
160
140
120
100
80
MASS NUMBER

Fig. 3

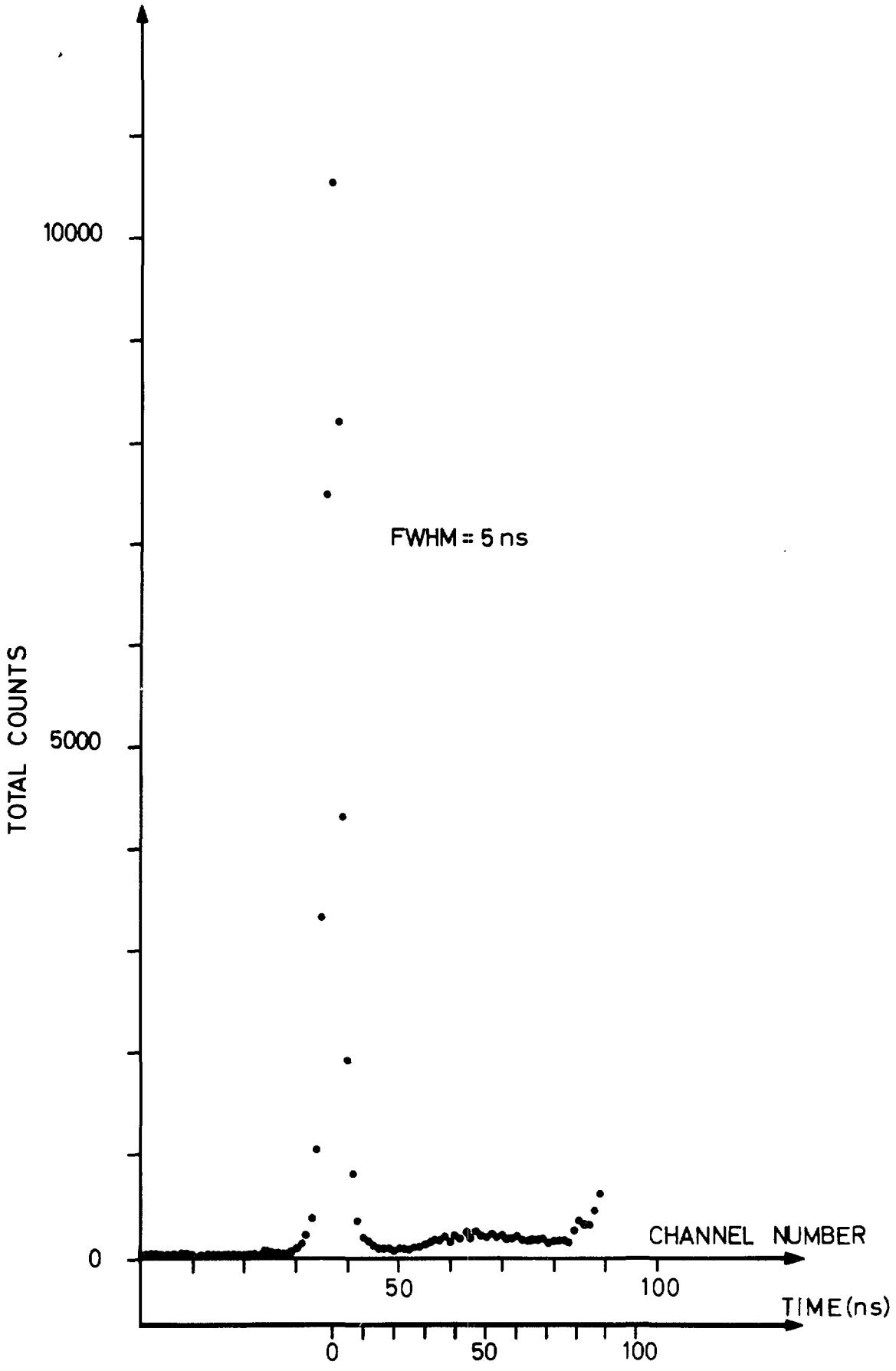
10000
5000
0
TOTAL COUNTS
FWHM = 5 ns
CHANNEL NUMBER
50
100
TIME(ns)
0
50
100

Fig. 4

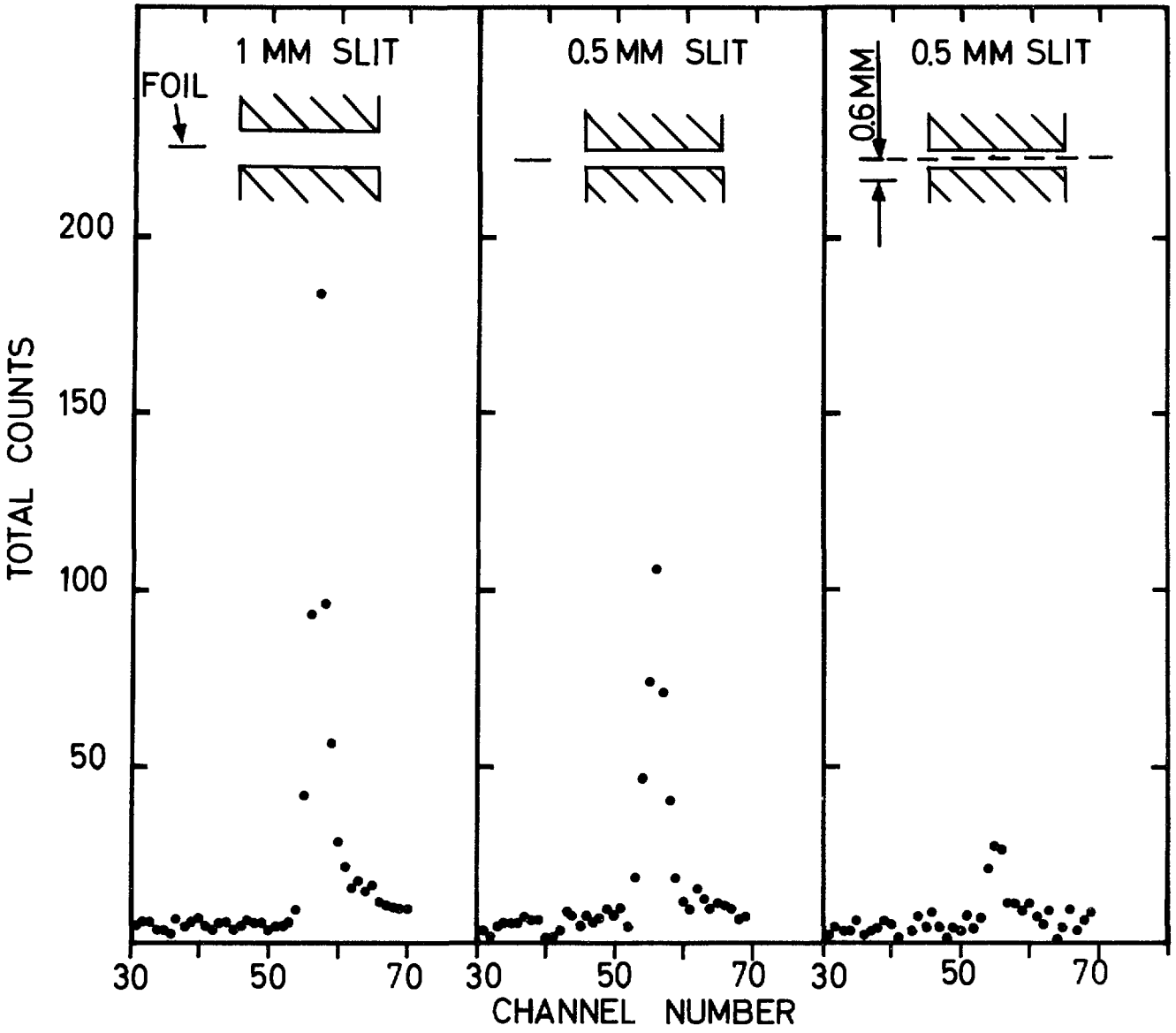
1 MM SLIT
FOIL
0.5 MM SLIT
0.6 MM
0.5 MM SLIT
TOTAL COUNTS
200
150
100
50
30
50
70
30
50
70
30
50
70
CHANNEL NUMBER

Fig. 5

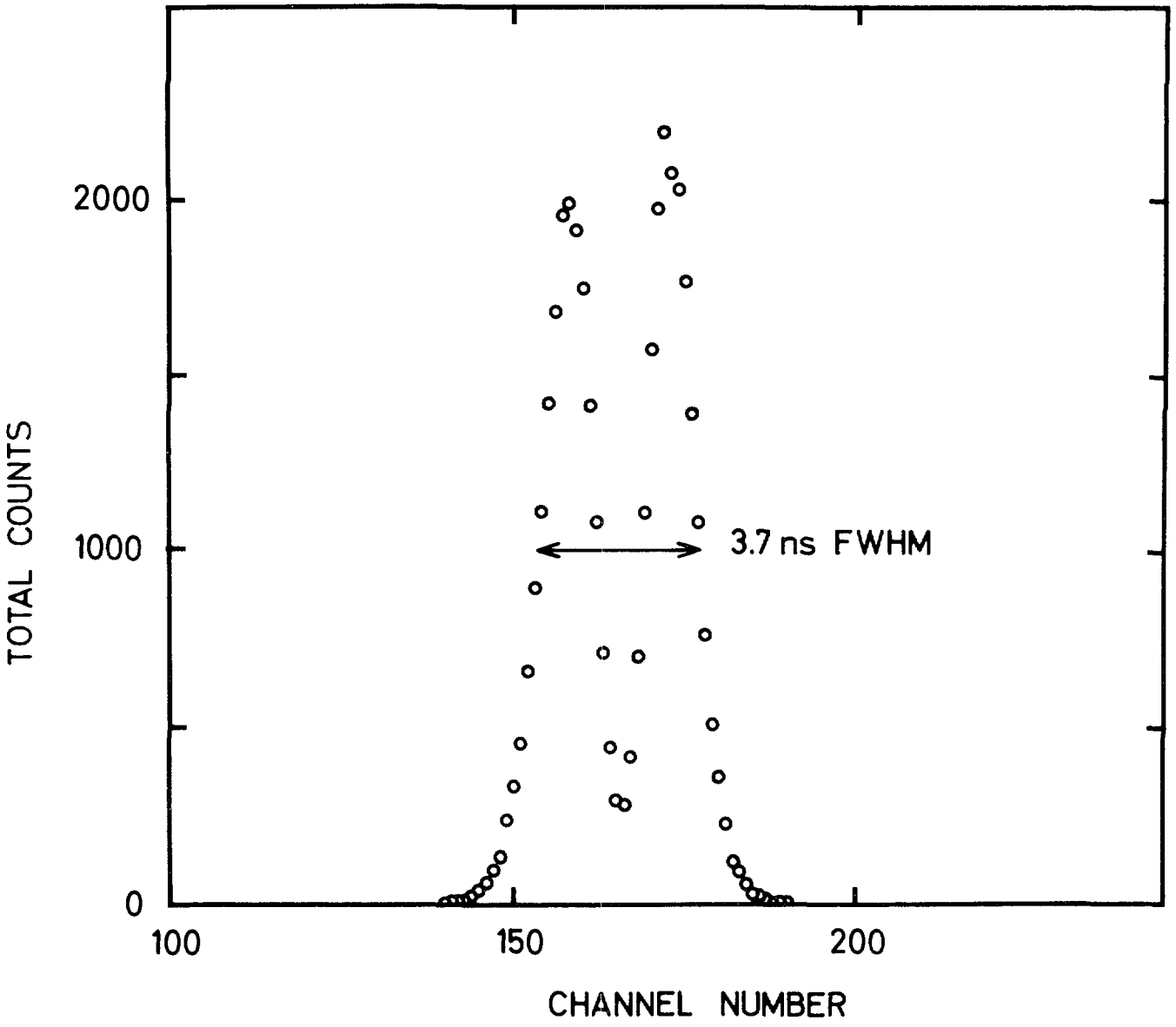
2000
1000
0
TOTAL COUNTS
3.7 ns FWHM
100
150
200
CHANNEL NUMBER

Fig. 6

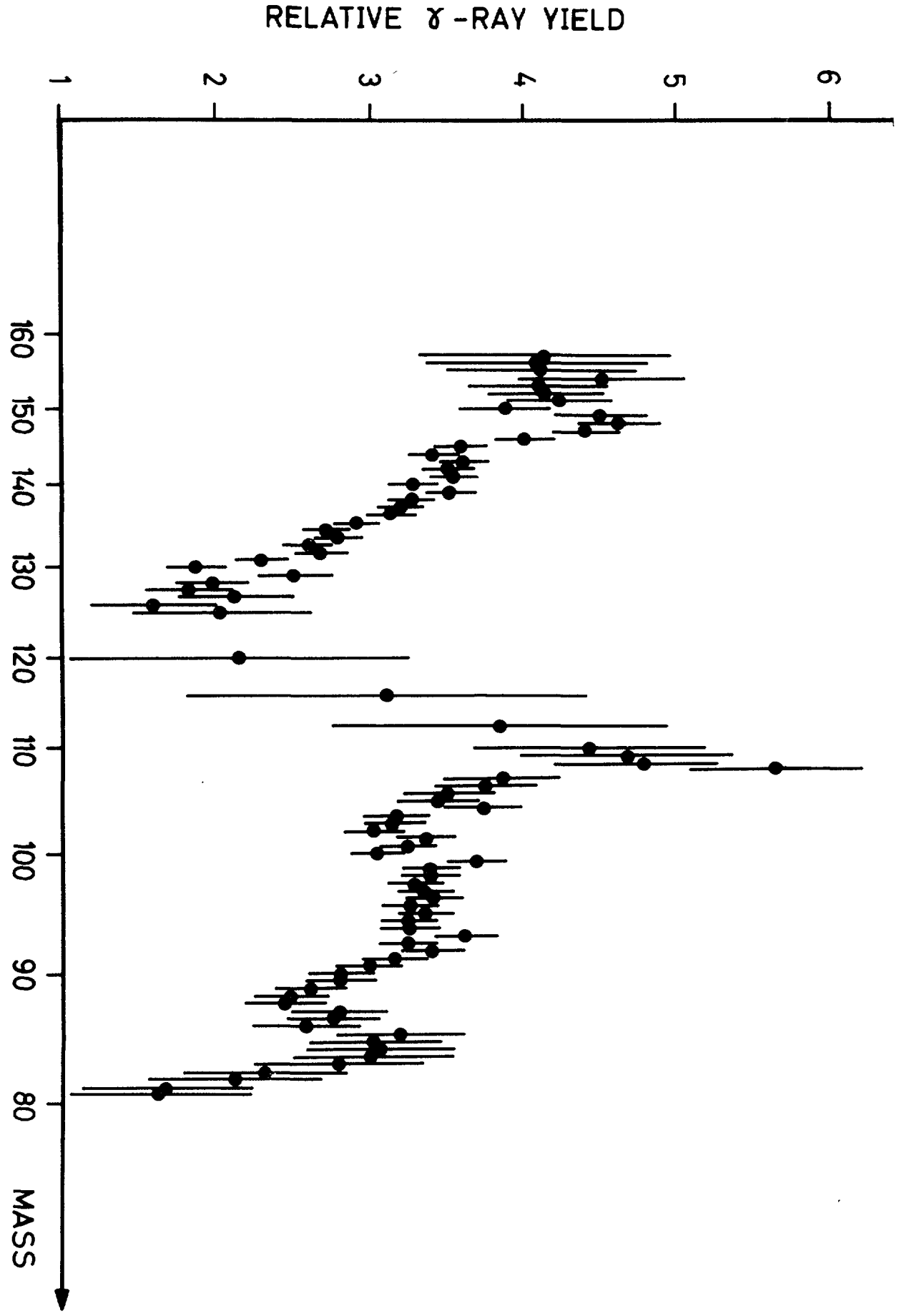
RELATIVE γ-RAY YIELD
1
2
3
4
5
6
160
150
140
130
120
110
100
90
80
MASS

Fig. 7

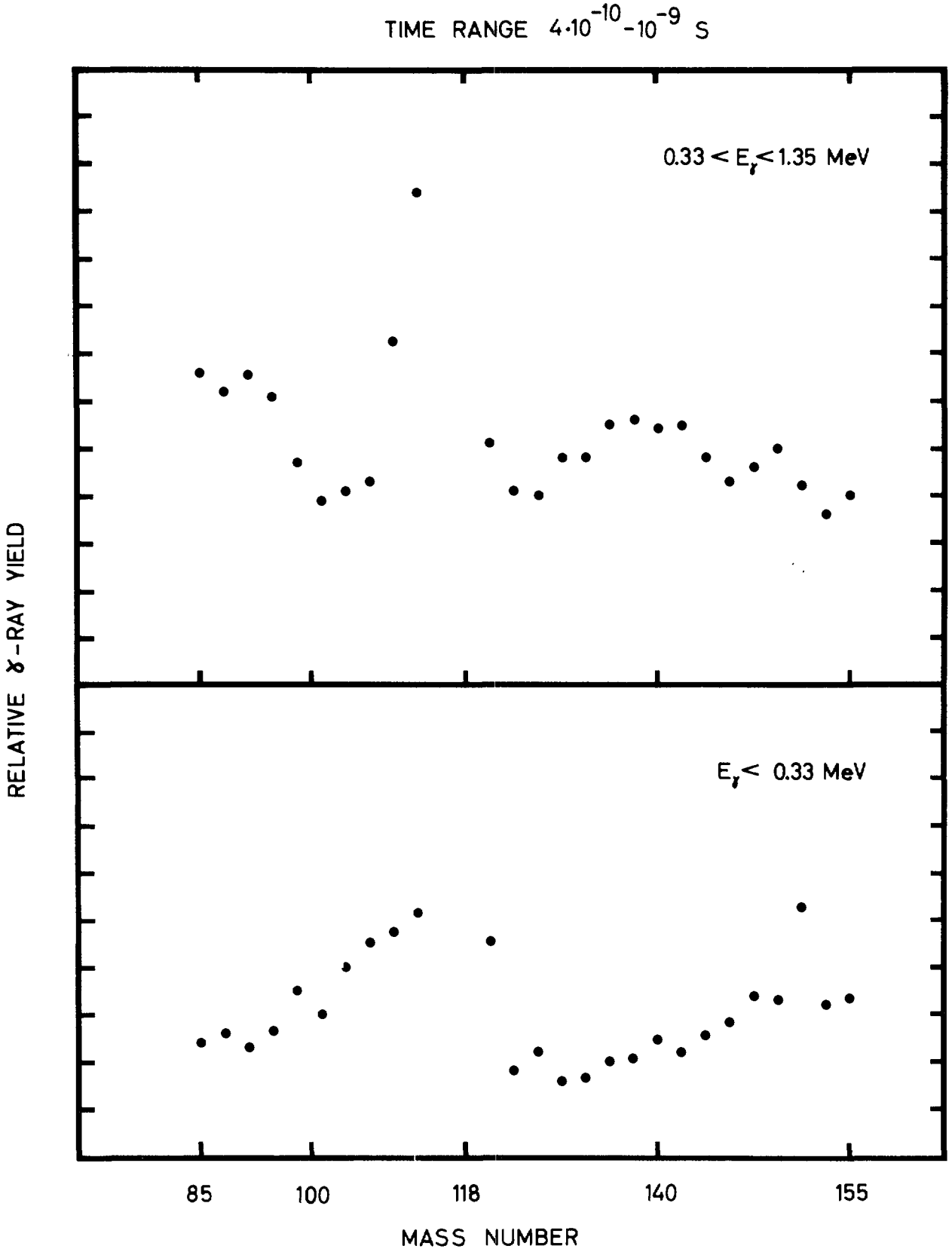
TIME RANGE $4 \cdot 10^{-10} - 10^{-9}$ S
$0.33 < E_\gamma < 1.35$ MeV
$E_\gamma < 0.33$ MeV
RELATIVE γ-RAY YIELD
85
100
118
140
155
MASS NUMBER

Fig. 8

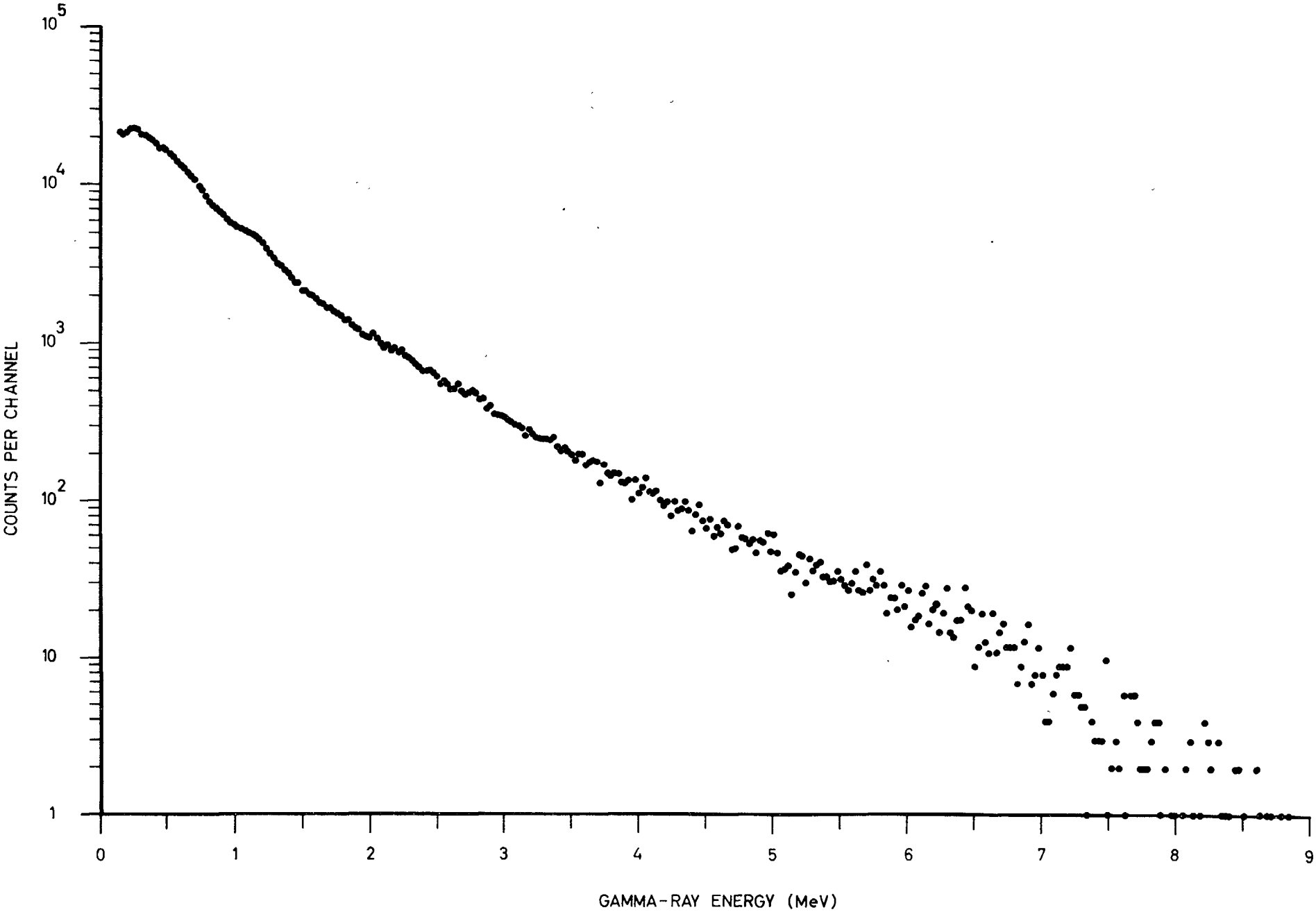
COUNTS PER CHANNEL
10^5
10^4
10^3
10^2
10
1
0
1
2
3
4
5
6
7
8
9
GAMMA-RAY ENERGY (MeV)

Fig. 9

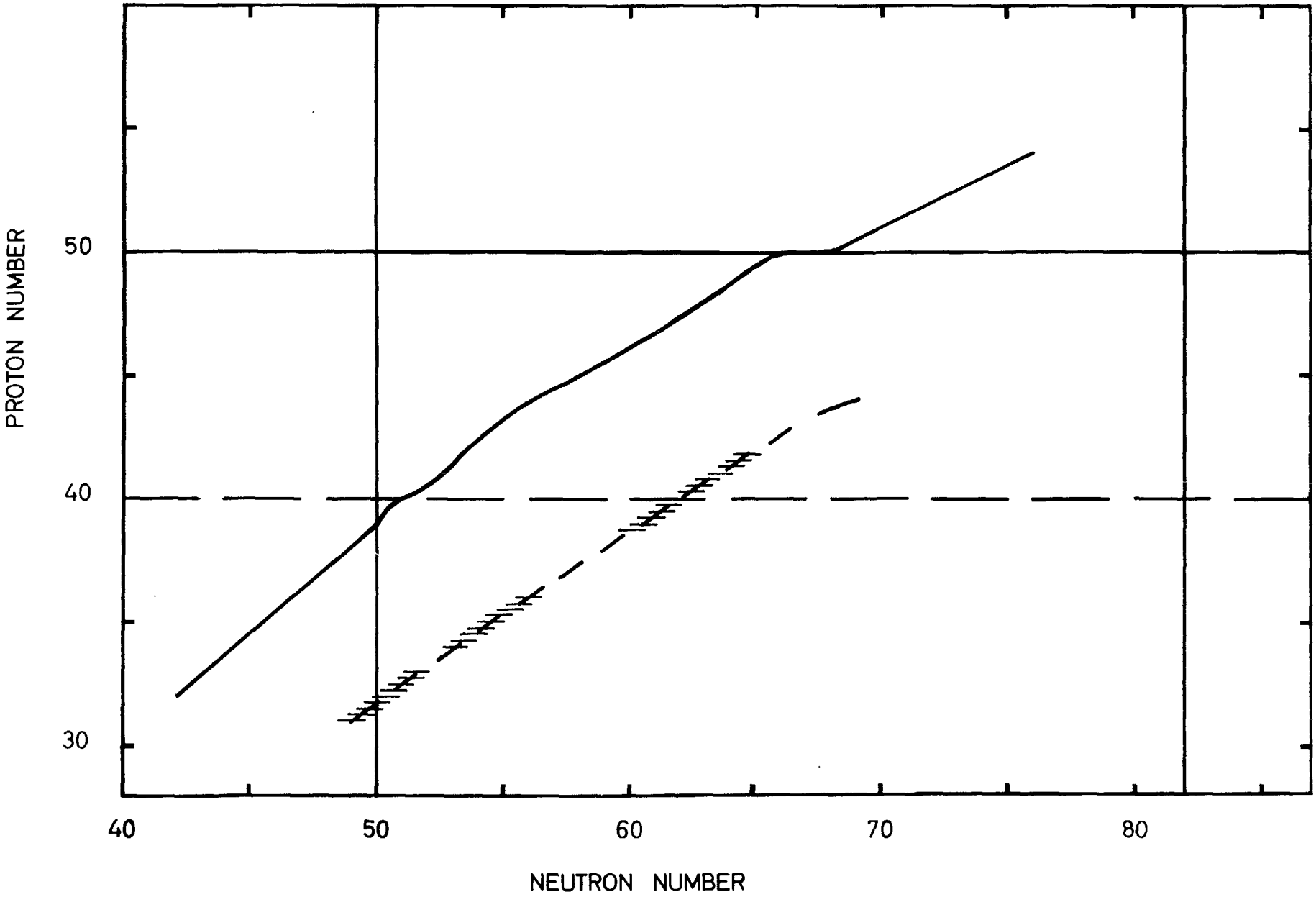

Fig. 10

LIST OF PUBLISHED AE-REPORTS

1–320 (See back cover earlier reports.)

321 Stability of a steam cooled fast power reactor, its transients due to moderate perturbations and accidents. By H. Vollmer. 1968. 36 p. Sw. cr. 10:–.

322. Progress report 1967. Nuclear chemistry. 1968. 30 p. Sw. cr. 10:–.

323 Noise in the measurement of light with photomultipliers. By F. Robben. 1968. 74 p. Sw cr. 10:–.

324. Theoretical investigation of an electrogasdynamic generator. By S. Palmgren. 1968 36 p. Sw. cr. 10:–.

325 Some comparisons of measured and predicted primary radiation levels in the Ågesta power plant. By E. Aalto, R Sandlin and A. Krell. 1968. 44 p. Sw cr. 10:–.

326. An investigation of an irradiated fuel pin by measurement of the production of fast neutrons in a thermal column and by pile oscillation technique. By Veine Gustavsson. 1968 24 p. Sw. cr. 10:–.

327. Phytoplankton from Tvären, a bay of the Baltic, 1961–1963. By Torbjörn Willén. 1968. 76 p Sw. 10:–.

328. Electronic contributions to the phonon damping in metals. By Rune Jonson. 1968. 38 p. Sw cr 10:–.

329. Calculation of resonance interaction effects using a rational approximation to the symmetric resonance line shape function. By H. Häggblom. 1968. 48 p. Sw. cr 10:–.

330. Studies of the effect of heavy water in the fast reactor FR0. By L. I Tirén. R. Håkansson and B. Karmhag. 1968. 26 p. Sw. cr. 10:–

331 A comparison of theoretical and experimental values of the activation Doppler effect in some fast reactor spectra By H. Häggblom and L. I. Tirén. 1968. 28 p. Sw. cr. 10:–.

332. Aspects of low temperature irradiation in neutron activation analysis. By D Brune. 1968. 12 p. Sw. cr. 10.–.

333. Application of a betatron in photonuclear activation analysis. By D. Brune, S. Mattsson and K. Lidén. 1968. 13 p. Sw. cr. 10:–.

334. Computation of resonance-screened cross section by the Dorix-Speng system. By H Häggblom. 1968. 34 p. Sw. cr. 10:–.

335. Solution of large systems of linear equations in the presence of errors A constructive criticism of the least squares method. By K. Nygaard. 1968 28 p. Sw cr 10:–.

336 Calculation of void volume fraction in the subcooled and quality boiling regions. By S. Z. Rouhani and E. Axelsson. 1968. 26 p. Sw. cr. 10:–.

337. Neutron elastic scattering cross sections of iron and zinc in the energy region 2.5 to 8.1 MeV. By B. Holmqvist, S. G. Johansson, A. Kiss, G. Lodin and T. Wiedling. 1968. 30 p. Sw. cr. 10:–.

338. Calibration experiments with a DISA hot-wire anemometer. By B. Kjellström and S. Hedberg. 1968. 112 p. Sw. cr. 10:–.

339 Silicon diode dosimeter for fast neutrons. By L. Svansson, P. Swedberg, C-O. Widell and M. Wik. 1968. 42 p. Sw. cr. 10:–.

340 Phase diagrams of some sodium and potassium salts in light and heavy water. By K. E. Holmberg. 1968 46 p. Sw. cr. 10:–.

341. Nonlinear dynamic model of power plants with single-phase coolant reactors. By H. Vollmer. 1968. 26 p. Sw. cr. 10:–.

342. Report on the personnel dosimetry at AB Atomenergi during 1967. By J Carlsson and T. Wahlberg. 1968. 10 p. Sw. cr. 10:–.

343 Friction factors in rough rod bundles estimated from experiments in partially rough annuli – effects of dissimilarities in the shear stress and turbulence distributions. By B. Kjellström. 1968. 22 p. Sw cr. 10:–.

344. A study of the resonance interaction effect between ^{238}U and ^{239}Pu in the lower energy region. By H. Häggblom. 1968. 48 p Sw. cr. 10:–.

345 Application of the microwave discharge modification of the Wilzbach technique for the tritium labelling of some organics of biological interest By T. Gosztonyi. 1968. 12 p. Sw. cr. 10:–.

346 A comparison between effective cross section calculations using the intermediate resonance approximation and more exact methods. By H. Häggblom. 1969. 64 p. Sw. cr. 10:–.

347. A parameter study of large fast reactor nuclear explosion accidents. By J. R. Wiesel. 1969. 34 p. Sw. cr. 10:–.

348 Computer program for inelastic neutron scattering by an anharmonic crystal. By L. Bohlin, I. Ebbsjö and T. Högberg. 1969. 52 p. Sw. cr. 10:–.

349. On low energy levels in ^{185}W. By S G. Malmskog, M. Höjeberg and V. Berg. 1969. 18 p. Sw. cr. 10:–.

350. Formation of negative metal ions in a field-free plasma. By E. Larsson. 1969. 32 p. Sw. cr 10:–.

351. A determination of the 2 200 m/s absorption cross section and resonance integral of arsenic by pile oscillator technique. By E. K. Sokolowski and R. Bladh. 1969. 14 p. Sw. cr. 10:–.

352. The decay of ^{191}Os. By S. G Malmskog and A. Bäcklin. 1969. 24 p. Sw cr 10:–.

353. Diffusion from a ground level point source experiment with thermoluminescence dosimeters and Kr 85 as tracer substance. By Ch. Gyllander, S Hollman and U Widemo. 1969. 23 p. Sw. cr. 10:–

354 Progress report, FFN, october 1, 1967 – september 30, 1968. By T. Wiedling. 1969. 35 p. Sw. cr. 10:–.

355. Thermodynamic analysis of a supercritical mercury power cycle. By A. S Roberts, Jr., 1969. 25 p Sw. cr. 10:–.

356. On the theory of compensation in lithium drifted semiconductor detectors By A. Lauber. 1969. 45 p. Sw cr 10:–.

357 Half-life measurements of levels in ^{75}As. By M. Höjeberg and S. G Malmskog. 1969. 14 p. Sw. cr. 10:–.

358. A non-linear digital computer model requiring short computation time for studies concerning the hydrodynamics of the BWR. By F. Reisch and G Vayssier. 1969. 38 p. Sw. cr. 10: –

359. Vanadium beta emission detectors for reactor in-core neutron monitoring. I. Ö. Andersson and B. Söderlund. 1969. 26 p. Sw. cr. 10:–.

360. Progress report 1968 nuclear chemistry. 1969. 38 p. Sw. cr. 10:–.

361. A half-life measurement of the 343.4 keV level in ^{175}Lu. By M. Höjeberg and S. G Malmskog. 1969. 10 p. Sw. cr. 10:–.

362 The application of thermoluminescence dosimeters to studies of released activity distributions. By B-I. Rudén. 1969. 36 p. Sw cr. 10:–.

363 Transition rates in ^{161}Dy. By V Berg and S. G. Malmskog. 1969. 32 p Sw. cr 10:–.

364. Control rod reactivity measurements in the Ågesta reactor with the pulsed neutron method. By K. Björeus 1969 44 p. Sw. cr. 10:–.

365. On phonons in simple metals II. Calculated dispersion curves in aluminium. By *R. Johnson and A. Westin.* 1969. 124 p Sw. cr. 10:–.

366. Neutron elastic scattering cross sections. Experimental data and optical model cross section calculations A compilation of neutron data from the Studsvik neutron physics laboratory. By B. Holmqvist and T. Wiedling. 1969. 212 p. Sw. cr 10:–.

367 Gamma radiation from fission fragments. Experimental apparatus – mass spectrum resolution. By J. Higbie. 1969. 50 p. Sw. cr. 10:–.

368. Scandinavian radiation chemistry meeting Studsvik and Stockholm, september 17-19, 1969. By H. Christensen. 1969. 34 p. Sw cr. 10:–.

369. Report on the personnel dosimetry at AB Atomenergi during 1968. By J Carlsson and T Wahlberg. 1969. 10 p. Sw. cr 10:–.

370. Absolute transition rates in ^{188}Ir. By S G. Malmskog and V. Berg. 1969. 16 p. Sw. cr. 10:–.

371. *Transition probabilities in the 1/2+(631) Band in* ^{235}U. By M. Höjeberg and S G Malmskog. 1969. 18 p. Sw. cr. 10:–.

372. E2 and M1 transition probabilities in odd mass Hg nuclei. By V. Berg, A. Bäcklin, B. Fogelberg and S. G Malmskog. 1969. 19 p. Sw. cr. 10:–.

373. An experimental study of the accuracy of compensation in lithium drifted germanium detectors. By A. Lauber and B. Malmsten. 1969. 25 p. Sw. cr. 10:–.

374. Gamma radiation from fission fragments. By J. Higbie. 1969. 22 p. Sw. cr. 10:–.

375 Fast Neutron Elastic and Inelastic Scattering of Vanadium. By B. Holmqvist, S. G. Johansson, G. Lodin and T. Wiedling. 1969. 48 p. Sw. cr. 10:–.

376. Experimental and Theoretical Dynamic Study of the Ågesta Nuclear Power Station. By P.-Å. Bliselius, H. Vollmer and F. Åkerhielm. 1969. 39 p. Sw. cr. 10: –

377. Studies of Redox Equilibria at Elevated Temperatures 1. The Estimation of Equilibrium Constants and Standard Potentials for Aqueous Systems up to 374°C. By Derek Lewis. Sw. cr. 10:-

378. The Whole Body Monitor HUGO II at Studsvik. Design and Operation. By L. Devell, I. Nilsson and L. Venner. 1970. 26 p. Sw. cr. 10:-.

379. ATOMSPHERIC DIFFUSION Investigations at Studsvik and Ågesta 1960–1963. By L-E Hæggblom, Ch Gyllander and U Widemo. 1969. 91 p. Sw. cr. 10: –

380. An expansion method to unfold proton recoil spectra. By J. Kockum. 1970. 20 p. Sw. cr. 10: –.

381. The 93. 54 keV level in ^{91}Sr, and evidence for 3-neutron states above N=50. By S. G. Malmskog and J. Mc Donald. 1970. 24 p. Sw. cr. 10:-.

382. The low energy level structure of ^{191}Ir. By S. G. Malmskog, V. Berg, A. Bäcklin and G. Hedin. 1970. 24 p. Sw. cr. 10:–.

383. The drinking rate of fish in the Skagerack and the Baltic. J. E. Larsson. 16 p. Sw. cr. 10: –.

384. Lattice dynamics of NaCl, KCl, RbCl and RbF. G. Raunio and S. Rolandson 26 p. Sw. cr. 10: –.

385 A neutron elastic scattering study of chromium, iron and nickel in the energy region 1.77 to 2.76 MeV. 26 p. By B. Holmqvist, S .G Johansson, G. Lodin, M. Salama and T. Wiedling. 1970. Sw. cr. 10: –

386. The decay of bound isobaric analogue states in ^{29}Si and ^{33}S using (d, nγ) reactions. By L. Nilsson, A. Nilsson and I. Bergqvist. 1970. 34 p. Sw. cr. 10:–.

387. Transition probabilities in ^{189}Os. By S. G. Malmskog, V. Berg and A. Bäcklin. 1970. 40 p. Sw. cr. 10: –.

388. Cross sections for high-energy gamma transitions from MeV neutron capture in ^{206}Pb. By I. Bergqvist, B. Lundberg and L. Nilsson. 1970. 16 p. Sw. cr. 10: –.

389 High-speed, automatic radiochemical separations for activation analysis in the biological and medical research laboratory. By K. Samsahl. 1970. 18 p. Sw. cr. 10: –.

390. Use of fission product Ru-106 gamma activity as a method for estimating the relative number of fission events in U-235 and Pu-239 in low-enriched fuel elements. By R. S. Forsyth and W. H. Blackadder. 1970. 26 p. Sw. cr. 10: –.

391. Half-life measurements in ^{134}I. By V. Berg and A. Höglund. 1970. 16 p. Sw. cr. 10: –.

392. Measurement of the neutron spectra in FR0 cores 5, 9 and PuB-5 using resonance sandwich detectors. By T. L. Andersson and M. N. Qazi. 1970. 30 p. Sw. cr. 10: –.

393. A gamma scanner using a Ge(Li) semi-conductor detector with the possibility of operation in anti-coincidence mode. By R. S. Forsyth and W. H. Blackadder. 1970. 22 p. Sw. cr. 10: –.

394. A study of the 190 keV transition in ^{141}La. By V. Berg, Å. Höglund and B. Fogelberg. 1970. 22 p. Sw. cr. 10:–.

395. Magnetoacoustic waves and instabilities in a Hall-effect-dominated plasma. By S. Palmgren. 1970. 20 p. Sw. cr. 10:–.

396. A new boron analysis method By J.Weitman, N.Dåverhög and S. Farvolden 26 p. Sw. cr. 10:-.

397. Progress report 1969. Nuclear chemistry. 39 p. Sw. cr. 10:–.

398. Prompt gamma radiation from fragments in the thermal fission of ^{235}U. By H Albinsson and L Lindow. 1970. 48 p. Sw. cr. 10:–.

List of published AES-reports (In Swedish)

1. Analysis be means of gamma spectrometry. By D. Brune. 1961. 10 p. Sw. cr. 6:–.
2. Irradiation changes and neutron atmosphere in reactor pressure vessels-some points of view. By M. Grounes. 1962. 33 p. Sw cr. 6:–.
3. Study of the elongation limit in mild steel. By G. Östberg and R. Attermo 1963 17 p Sw. cr. 6:–.
4. *Technical purchasing in the reactor field.* By *Erik Jonson.* 1963. 64 p. Sw. cr. 8:–.
5. Ågesta nuclear power station. Summary of technical data, descriptions, etc. for the reactor. By B Lilliehöök. 1964. 338 p. Sw cr. 15:–.
6. Atom Day 1965. Summary of lectures and discussions. By S. Sandström. 1966. 321 p. Sw. cr. 15:–.
7. Building materials containing radium considered from the radiation protection point of view. By Stig O W. Bergström and Tor Wahlberg. 1967. 26 p. Sw cr. 10:–.

Additional copies available from the library of AB Atomenergi, Fack, S-611 01 Nyköping, Sweden.

EOS-tryckerierna, Stockholm 1970